Low-Profile Dual Hollow Octagonal Ring Shaped Optically Transparent Tri-band Antenna for WLAN and Sub-6 GHz 5G Applications

Pankti SHAH[1], *Yesha PATEL*[1], *Arpan DESAI*[1,*], *Trushit UPADHAYAYA*[1], *Merih PALANDOKEN*[2]

[1]Department of Electronics and Communication Engineering, CSPIT, CHARUSAT, Charotar University of Science and Technology (CHARUSAT), Changa 388421, India
[2]Department of Electrical and Electronics Engineering, Faculty of Engineering and Architecture, İzmir Katip Çelebi University, İzmir, Turkey

*Corresponding Author: Arpan DESAI (Email: arpandesai.ec@charusat.ac.in)
(Received: 13-Jun-2021; accepted: 30-Jul-2021; published: 30-Sep-2021)
DOI: http://dx.doi.org/10.55579/jaec.202153.336

Abstract. *A transparent dual octagonal split ring-shaped resonator connected by a horizontal strip is proposed for tri-band applications. Stub-loaded microstrip line fed structural design of radiator consists of two slotted octagonal-shaped rings connected via a strip on the top with the partial ground at the back. The low profile (40×25 mm^2) radiator achieves impedance bandwidth of (46.08%) 1.62-2.59, (7.78%) 3.95-4.27, and (12.60%) 5.13-5.82, respectively. A bi-directional (dipole shaped) radiation pattern with maximum gain and minimum efficiency of 2.5 dBi and 52%, respectively is achieved. Transparency above 80%, low profile structure, and tri-band operation make the antenna a good contender for WLAN and Sub-6 GHz 5G applications. Good correlation is observed for the modeled and experimental parameters.*

Keywords

Transparent, split-ring, multiband, 5G, WLAN.

1. Introduction

Wireless Communication has become a crucial part of today's era of 4G and 5G technology. Transmitting information through the air medium with the help of electromagnetic waves to wireless devices can be ameliorated with the help of antennas. Wireless technology allows people to work from remote locations for several applications which rises the demand for compact, multiband, and easy to establish antennas that leads to seamless connectivity. The need has elevated due to advancements in electronics gadgets with multiple usabilities.

Many designs of antennas have been proposed for achieving multiband antennas. Among them, the applications covering WLAN (Wireless Local Area Network) and sub-6 GHz band is in very much demand. The antenna usability can be further increased if the antennas are made transparent as they can be interfaced anywhere without causing any visual clutter. The main idea behind making the antenna transparent is that it can be installed everywhere without caus-

ing any visual clutter and it also helps in receiving the signals at every possible corner. There - two main categories include mesh [1] and conductive oxide [2] based antennas. Mesh structures can easily be detected while antennas are made up of oxides like FTO (Fluorine Tin Oxide), ITO (indium Tin Oxide), AgHT (Silver Tin Oxide), AZnO (Aluminum Doped) achieves completely transparency. Such antennas can be prepared from commercially available sheets or sputtering techniques [3], and the chemical vapor deposition process [4]. Due to the easy availability of AgHT-8 in the form of sheets along with sheet impedance of 8Ω/Sq, it is widely acceptable for fabrication of transparent antennas Multiband transparent antennas can be useful for better signal quality by attaching it to indoor ceilings and walls, window glasses, large monitors, and automobile glazing due to their unobtrusive property.

Various tri-band antennas are proposed in the literature for wireless applications [5]-[18]. A compact triple-band antenna that is made reconfigurable with the use of a PIN diode in the external split ring of the metamaterial structure is proposed in [5] that covers WiMAX and WLAN band. In [6] a Tri-band Y shaped slotted monopole antenna with a Split-Ring meandering slot and a symmetrical upturned L-strips pair having steady gain and the broadside radiation pattern is presented that span from (2.33–2.76 GHz), (3.05–3.88 GHz), and (5.57–5.88 GHz). A monopole tri-band antenna with a feeding element such as a coplanar waveguide covers the 2.4/5 GHz WLAN and 3.5/5 GHz WiMAX is proposed. It can cover more bandwidth in comparison with [5]. The radiator consists of an S-shaped strip and a rectangular ring, with a U-shaped strip in a crooked manner and a bottom layer with three strips [7]. A revised structure named compact triband printed antenna which works for 2.4,3.5,5 GHz is proposed in [8]. The size of the antenna is $17\times23.5\times1.6$ mm^3 whereas it is capable to cover 2.4,5.2,5.8 GHz and 3.5,5.5 GHz. Bandwidth coverage ameliorated in comparison with [5]-[7]. The number of antennas used in [6] and [8] is the same but [8] has a more strip-based structure which makes its structure less complex. Amalgamating the different communication systems into a single antenna system is made with the implementation of the triple-band antenna with an E-plane coupled MSA antenna having two elements with a defected base having a size of $50\times50\times1.6$ mm^3 [9]. A polarised antenna with a Y-shaped radiating element and partial ground with monopole arms is circularly polarised having a dimension of 35×45 mm^2 [10]. A circular slot-loaded compact cylindrical tri-band dielectric resonator antenna working in the 2.4/5.2 and 3.5 GHz regimes [11] with a similar size of the antenna as [9] is proposed. An integrated antenna system for WiGig (57 to 64 GHz) and WLAN (2.4 to 2.485 GHz and 5.15 to 5.85 GHz) and application based on magnetic electric dipole and a stacked patch antenna has been developed with a large frequency ratio however it suffers from huge bandwidth difference in certain applications [12]. A rectangular tri-band antenna is designed for an application covering WiMAX and WLAN, that received problems while fabricating small shorts without the presence of air and got 0.8 GHz deviation w.r.t simulated results [13]. Although, it exhibits multi-band matching but does have a complex structure. Similarly, a compact metamaterial reconfigurable antenna illustrated in [14] covers 2.4, 3.5, and 5 GHz, bands. A triple-band MIMO antenna with omnidirectional radiation pattern with measured radiation gain of 0.253, 0.6, and 3.38 dBi at 0.9, 1.8, and 2.6 GHz with low correlation coefficient and covers GSM900/1800 and LTE2600 bands is proposed in [15]. Nonuniform fork and meandered type grounded radiator works on a triple band which is capable of covering the WLAN band with good radiation pattern and impedance matching [16]. A slot-loaded microstrip multi-band antenna with a defected ground base has been designed for the IoT applications which resonated in 2.42, 5.22, and 5.92 GHz bands [17]. Subsequently, in this smart world GSM, Bluetooth and DCS are stated under the rudimentary categories where the antenna transmission and reception play a vital role for access in rural and urban zones. An inverted F-antenna in a folded planar is capable of covering GSM, DCS, and Bluetooth bands [18].

There are few more tri-band antennas which are proposed for WLAN-WiMAX [19], UAV [20],

multi-standard terminals [21], notebook computers [22], and beam scanning [23] applications.

However, the antennas proposed above are non-transparent and both WLAN with sub-6 GHz bands are still not covered. In [25]-[27], transparent antennas with dual-band [25] and tri-band [26, 27] is presented. The transparent antenna in [25], is a slotted split ring resonator with the slot line extended to the patch which covers bands of 2.4 and 5.26 GHz, respectively. It is capable of indoor WLAN applications whereas the opaqueness issue has been raised. In [26], a flexible transparent antenna is proposed for GSM, WiMAX, WLAN, 3G, 4G, and 5G applications however flexible antennas often suffer from low efficiency and gain due to the thin substrate and bending conditions.

In this work, a compact antenna having dual octagonal-shaped rings connected with a horizontal strip is proposed. Transparency above 80%, low profile structure, and tri-band operation make the antenna a good contender for WLAN and Sub-6 GHz 5G applications. The satisfactory agreement between the measurement and numerical computations of RF performance indicates the technical potential of an octagonal ring-shaped transparent antenna for interfacing the antenna in devices using WLAN and sub-6 GHz 5G applications.

2. Antenna configuration and design geometry

The transparent antenna models' top, side, and 3-D view are depicted in Fig. 1. The blending of the transparent substrate and conductive sheet helps the antenna in achieving transparency more than 85%. The lightweight transparent structure consists of a Plexiglas (thickness = 1.48 mm, dielectric constant (εr) = 2.3 and tan δ = 0.003) that serves as a substrate and AgHT-8 (silver tin oxide) as patch and ground material, respectively. AgHT-8 is a thin transparent sheet (thickness = 0.177 mm and surface resistance of 8 Ω/m). Antenna geometry consists of two octagonal splits ring-shaped structures with slots that are united using a rectangular strip is interfaced with a stub-loaded microstrip feed-line on the top and partial ground on the bottom. A transparent antenna accomplishes a size of 40×25 mm^2. The fabricated transparent antenna model is illustrated in Fig. 2. An adhesive sheet (thickness=0.19 mm) is utilized for interfacing the conductive sheet and substrate. The 50Ω SMA is connected using conductive epoxy with a feed line to avoid hot solder.

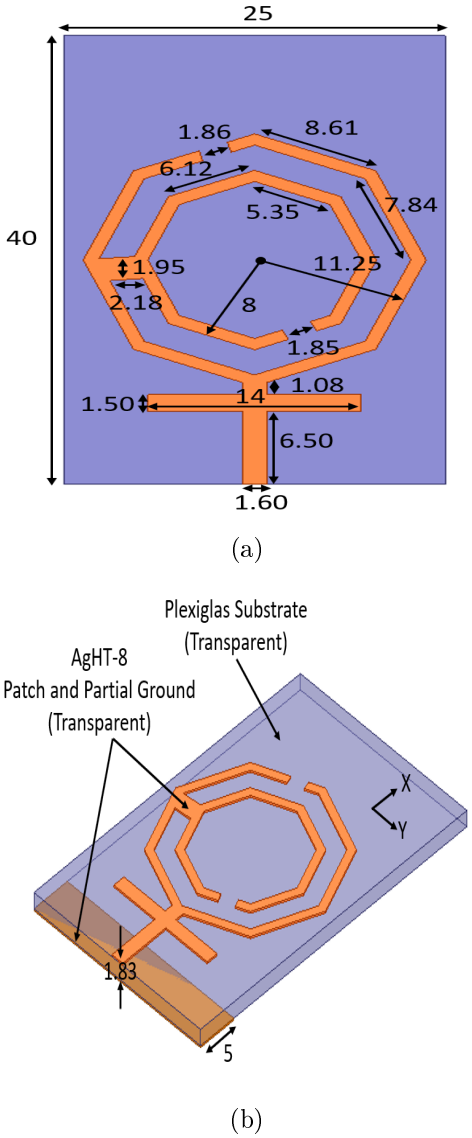

Fig. 1: Antenna Geometry (a)Top View (b) Perspective View (Dimension in mm).

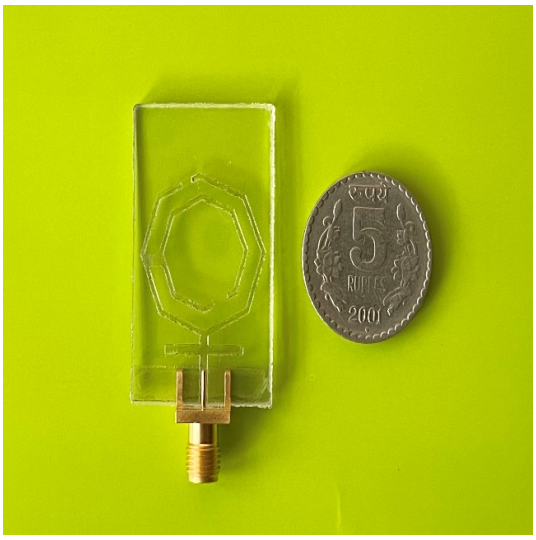

(a)

(b)

Fig. 2: Fabricated Prototype (a) Top View (b) Front View.

3. Parametric analysis

The antenna has been designed with disparate radii in the octagonally shaped ring on the top and partial ground on the bottom. The base antenna consists of a solid octagonal-shaped patch and full ground. Subsequently, the six consecutive changes are carried out for achieving the required bands resonating in WLAN and sub-6 GHz 5G. Firstly, the octagonal ring with a narrow strip and a slot has been made which is

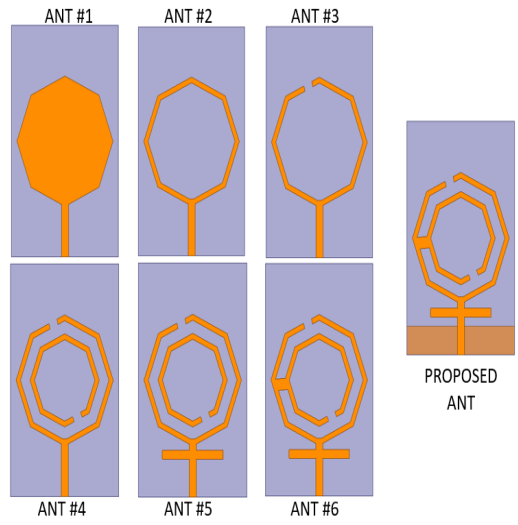

Fig. 3: Antenna Evolution Process.

illustrated as antenna 1 and 2 in Fig. 3. Conjunction with the outer ring, a second octagonal slotted ring is added to form antenna 4. A horizontal strip is added to attach the two slotted octagonal-shaped rings. The slots of the ring are oriented in opposite directions to avoid the internal collision of radiations. Finally, in the proposed design, the ground plane is made partial which is elucidated in Fig. 3.

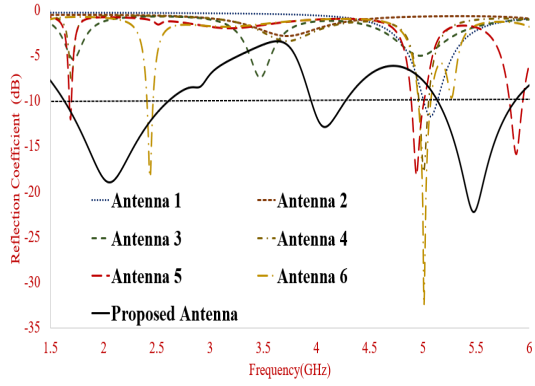

Fig. 4: Reflection Coefficient of Antenna Evolution Process.

While tuning Antenna 1 with a full ground plane it is having a steady reflection coefficient mainly. This rudimentary antenna radiates at 5 GHz with a normal reflection value which cannot be used omnipotently. Consecutively, the octagonal antenna with a filled pattern has been

transformed to a simple narrow octagonal ring (antenna 2). Antenna 2 has the languishing effect in comparison with the previous antenna with approximately -3 dB reflection coefficient. Revised Antenna 3 with a slight gap in the ring shows the improvised value of reflection coefficient but not up to the mark. Subsequently, Antenna 4 with the second octagonal ring has been placed with lesser radii than the outer ring. The gap in the outer ring directs in the upper direction and the gap in the second ring directs towards down which establishes the reflection coefficient value below -15 dB which is considerable. Antenna 5 with horizontal strip elevates the performance of the model which results in radiation spikes below -10 dB. To further improve the radiation, the interconnection of the two octagonal rings has been made. Antenna 6 with improvised structure have dual-band performance with reflection coefficient spike at -34 dB which still lacks the required impedance bandwidth for WLAN operation whereas the sub-6 GHz band is still not covered. Thus, the final antenna is proposed with the partial ground plane, which radiates at WLAN and sub-6 GHz band with a reflection coefficient below -10 dB. The partial ground is added at the last since the defected ground structure is known to improve the impedance bandwidth of the resonant frequency and so it was not added from the very first stage. The antenna was first optimized to work at dual-band covering both the WLAN bands but to improve the impedance bandwidth, the partial ground was added instead of full ground. In doing so the impedance bandwidth did improve significantly while achieving an additional band between the previously attained bands.

To understand the working of the antenna, parametric analysis is performed to analyze the effect on the reflection coefficient. The outer ring thickness (ORT) is varied where it can be observed that when the thickness increases, the frequency band shifts towards the higher side whereas a decrease in the thickness leads to shifting in the first and second resonant frequency towards the lower side as shown in Fig. 5(a). The optimum value of 0.93 mm is chosen as the thickness. In Fig. 5(b), the reflection coefficient is observed by changing the inner ring thickness (IRT). As the value of IRT increases, the frequency at the third resonant shifts towards the higher side of the band while there is no significant change in the other two bands.

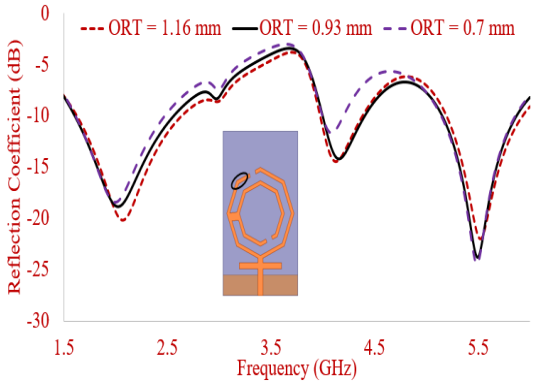

(a)

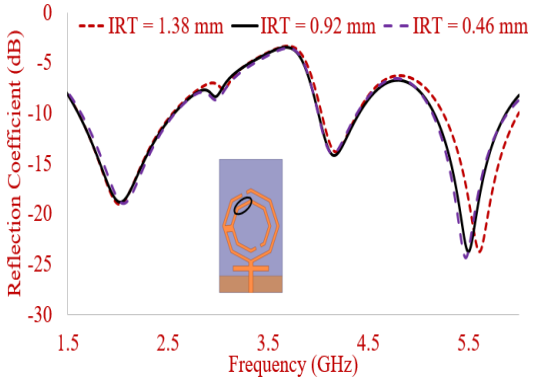

(b)

Fig. 5: Variation in terms of (a) Outer Ring Thickness (ORT) (b) Inner Ring Thickness (IRT).

Figure 6(a) illustrates the effect on the reflection coefficient due to variation of the slot length (SL). Significant effect on the second and third band is observed in terms of impedance bandwidth and reflection coefficient when the slot length is increased or decreased however the first band is least affected due to the same. The effect on the reflection coefficient by rotating the connector (C) connecting the outer and inner octagonal ring is observed in Fig. 6(b). When the connector is rotated from the 5^0 position towards the 0^0 position, the impedance bandwidth at the second and third band significantly improved however the third resonant band shifted

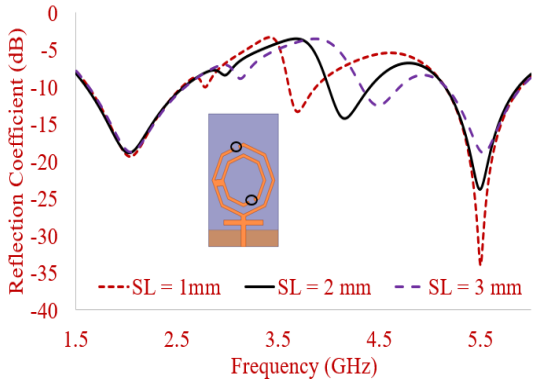

(a)

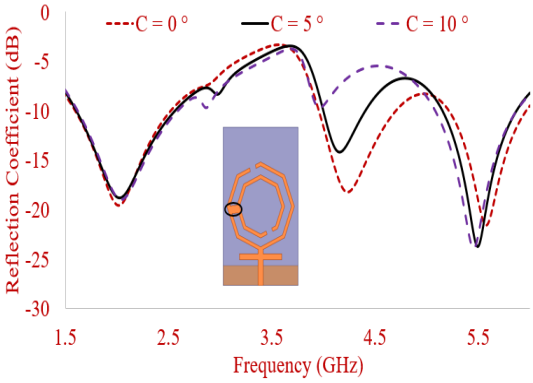

(b)

Fig. 6: Variation in terms of (a) Outer and Inner Ring Slot Length (SL) (b) Outer and Inner Ring Connector Position (C).

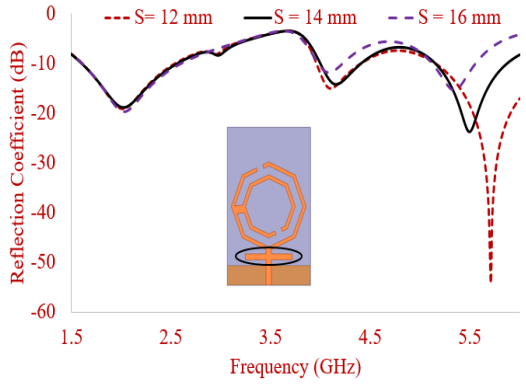

(a)

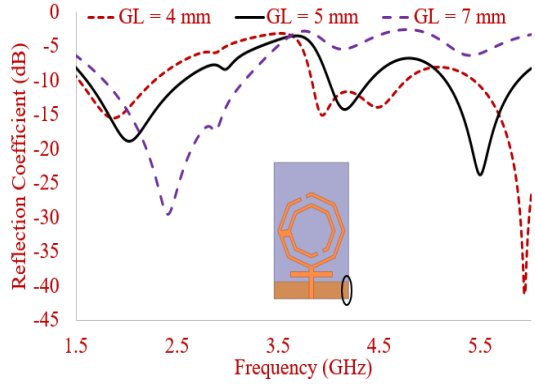

(b)

Fig. 7: Variation in terms of (a)Stub Size (S) (b) Ground Length (GL).

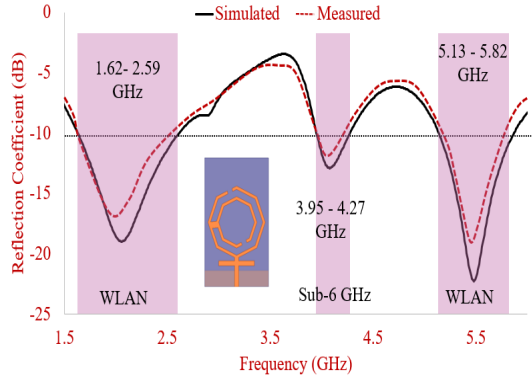

Fig. 8: Reflection Coefficient Plot.

a bit more towards the higher side thus deviating from the bands of interest (WLAN). While the rotation to 10^0 led to only dual-band performance. The connector position is selected as 5^0 as the same covers the required band and attains acceptable impedance bandwidth.

The effect of the stub length variation (S) is depicted in Fig. 7(a) where it is observed that optimum stub length helps in achieving the right level of reflection coefficient while improving the impedance bandwidth as well. The stub length of 14 mm is selected as the same achieve the required frequency bands with superior IBW compared to other results. Finally, the length of the ground plane (GL) has been varied which plays a vital role in establishing the required impedance bandwidth of the tri-band transparent antenna. The best performance is observed for length of the ground = 5 mm as tri-band performance is

observed along with the satisfactory values of the impedance bandwidth as shown in Fig. 7(b).

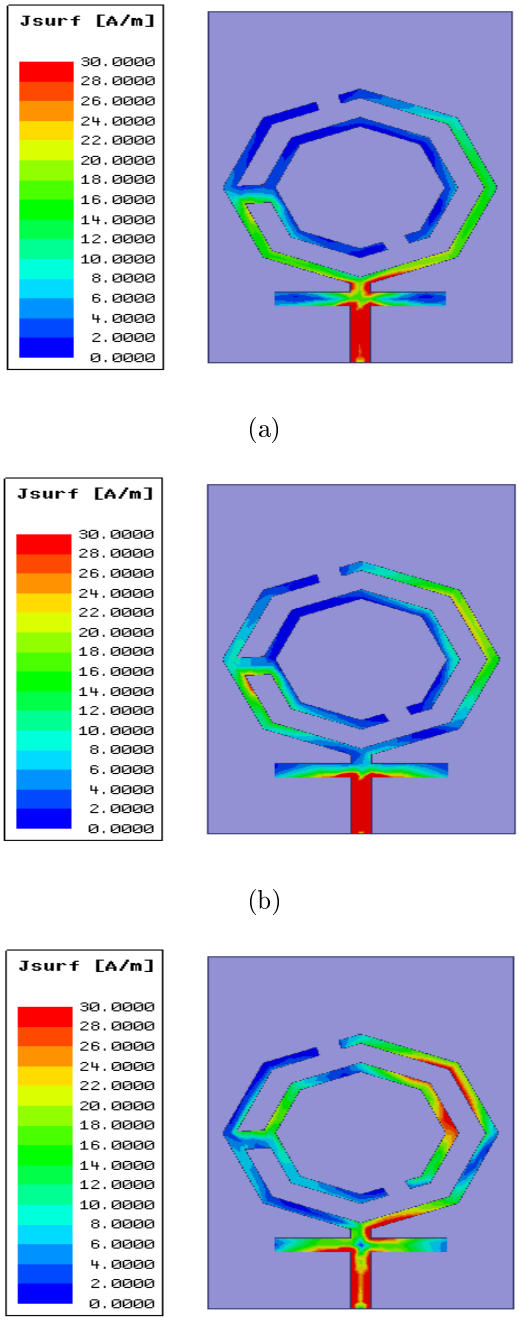

Fig. 9: Current Distribution at (a) 2.05 GHz (b) 4.08 GHz (c) 5.47 GHz.

4. Results and discussion

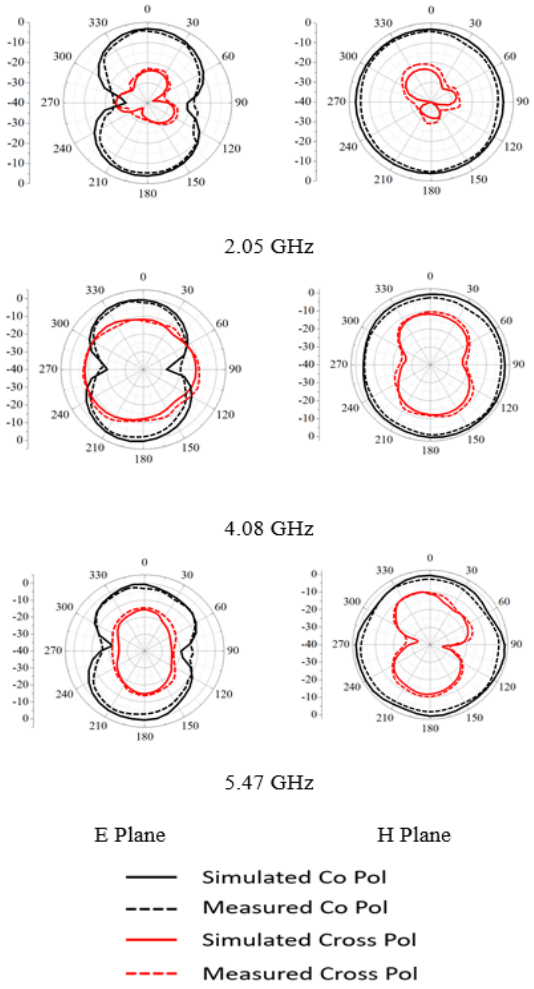

Fig. 10: 2-D Co/Cross Pol Radiation Pattern.

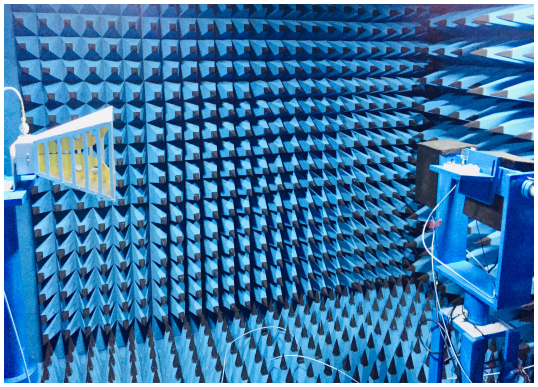

Fig. 11: Radiation Pattern Measurement Setup in Anechoic Chamber.

Tab. 1: Comparison of Transparent Tri-band Antenna Performance with other multiband antennas.

Ref No.	Operating freq. (GHz)	Substrate/ Transparent	Gain (dB)	Size (mm^2)	Ground Plane
Ref. [6]	2.5/3.5/5.5	FR4/ No	-2/1.5/1	18×33	Modified CPW Fed
Ref. [8]	2.4/5/3.5/5.5	FR 4/ No	1.85/1.87/2.80	17×23.5	Asymmetric trapezoid
Ref. [12]	2.4/5/60	Rogers 5880/ No	9.8/7.9/8.4	1.12×1.12	Square-shape with box type reflector and shorting pin with an air gap
Ref. [16]	2.40-2.484/ 5.150-5.350/ 5.725-5.825	FR 4/ No	1.48/2.30/ 3.05	34×8	Fork-shape
Ref.[17]	2.42/5.22/5.92	Rogers RO3003/ No	2.48/7.17 /8.18	55.5×42.75	Split rings shape defected ground
Ref. [18]	0.89/1.8/2.4	FR 4/ No	1.47/2.05 /2.37	30×12	Ground with shorting pin and airgap
Ref. [25]	2.42/3.7 (2×1 array)	Plexiglas/ Yes	1.98/2.95	105×60	Rectangular shaped Partial Ground
Ref. [26]	0.88-1.03/ 1.47-2.74/ 3.32-5.97	Glass/ Yes	-0.18/3.66/4.35	60×40	Slotted Rectangular shaped Partial Ground
Ref. [27]	2.45/3.8/5.7	Polyimide/ Yes	3.27/9.47/4.47	30×30	Rectangular shaped Partial Ground
Proposed work	2.05, 4.08 and 5.47 GHz	Plexiglass/ Yes	1.1/1.9/2.5	40×25	Rectangular shaped Partial Ground

The radiator is fabricated and tested using a Keysight handheld N9915A vector network analyzer and anechoic chamber after carrying out numerical computations and optimization in commercial 3D electromagnetic field solver software, Ansoft. The reflection coefficient results are illustrated in Fig. 8 for the proposed design. It is observed that the simulated antenna achieves tri-band resonance at (46.08%) 1.62-2.59, (7.78%) 3.95-4.27, and (12.60%) 5.13-5.82 which closely matches the measured values. The measured impedance bandwidth is slightly lower due to the tolerances in geometric fabrication and calibration errors in RF cabling-based systems.

The distribution of current in the octagonal-shaped transparent antenna at 2.05, 4.08, and

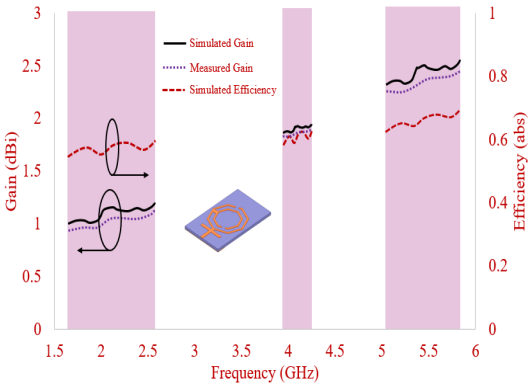

Fig. 12: Frequency Variation in terms of Gain and Efficiency.

5.47 GHz is presented in Fig. 9. At 2.05 GHz, the distribution of current is observed on the stub, outer ring, and the strip connecting inner and outer hollow octagonal-shaped rings. Very little current is coupled in the inner ring whereas, at 4.08 GHz, the current is also coupled with the inner ring where major distribution is observed on the sides next to the slotted regions. At 5.47 GHz, the majority of the surface current is observed near the right edges of inner and outer octagonal rings.

The 2D co/cross-polarization patterns of the transparent radiator along the E and H plane are depicted in Fig. 10 which is numerically calculated using HFSS software and experimentally measured in an anechoic chamber as illustrated in Fig. 11. At least a 10 dB difference between co and cross-pol pattern is observed which is true for both simulated and measured results. At the E plane bidirectional (dipole shaped) pattern is achieved while at the H plane, the omnidirectional pattern is observed.

Figure 12 portrays the gain and efficiency of the proposed low-profile transparent antenna. The simulated gain of the antenna is 1.1, 1.9, and 2.5 dBi at 2.05, 4.08, and 5.47 GHz where efficiency ranges from 58-67%, respectively. The measured gain demonstrated well correlation with the simulated results.

The performance comparison of the low-profile tri-band transparent antenna with other antennas is carried out as shown in Tab. 1. The antenna radiates at WLAN and sub-6 GHz band, with the satisfactory value of reflection coefficient, peak gain, and achieves more than 80% optical transparency.

5. Conclusions

A low-profile transparent antenna with disparate radii in the octagonally shaped ring on the top and partial ground on the bottom is proposed. The optimized antenna geometry helped in achieving tri-band performance spanning from (46.08%) 1.62-2.59, (7.78%) 3.95-4.27, and (12.60%) 5.13-5.82, gain greater than 1 dBi and bidirectional pattern at bands of interest. The triband resonance attainment and design process are backed by numerical computations, parametric studies, and experimental results. The antenna exhibits more than 80% transparency and compact size that makes it suitable for its placement in the indoor or outdoor facility without being noticed. Thus, it offers seamless connectivity to the devices working on WLAN and sub-6 GHz frequency.

References

[1] Turpin, T. W., & Baktur, R. (2009). Meshed patch antennas integrated on solar cells. *IEEE Antennas and Wireless Propagation Letters, 8*, 693-696.

[2] Ginley, D. S., & Bright, C. (2000). *Transparent conducting oxides. MRS bulletin, 25*(8), 15-18.

[3] Wu, C. T., Ho, Y. R., Huang, D. Z., & Huang, J. J. (2019). AZO/silver nanowire stacked films deposited by RF magnetron sputtering for transparent antenna. *Surface and Coatings Technology, 360*, 95-102.

[4] Azuma, K., Ueno, S., Konishi, Y., & Takahashi, K. (2015). Transparent silicon nitride films prepared by surface wave plasma chemical vapor deposition under low temperature conditions. *Thin Solid Films, 580*, 111-115.

[5] Rajeshkumar, V., & Raghavan, S. (2015). A compact metamaterial inspired

triple band antenna for reconfigurable WLAN/WiMAX applications. *AEU-International Journal of Electronics and Communications, 69*(1), 274-280.

[6] Liu, P., Zou, Y., Xie, B., Liu, X., & Sun, B. (2012). Compact CPW-fed tri-band printed antenna with meandering split-ring slot for WLAN/WiMAX applications. *IEEE Antennas and Wireless Propagation Letters, 11*, 1242-1244.

[7] Xu, Y., Jiao, Y. C., & Luan, Y. C. (2012). Compact CPW-fed printed monopole antenna with triple-band characteristics for WLAN/WiMAX applications. *Electronics Letters, 48*(24), 1519-1520.

[8] Osklang, P., Phongcharoenpanich, C., & Akkaraekthalin, P. (2019). Triband compact printed antenna for 2.4/3.5/5 GHz WLAN/WiMAX applications. *International Journal of Antennas and Propagation, 2019*.

[9] Surendrakumar, P., & Mohan, B. C. (2018). A triple-frequency, vertex-fed antenna for WLANWiMAX applications [antenna applications corner]. *IEEE Antennas and Propagation Magazine, 60*(3), 101-106.

[10] Wu, T., Shi, X. W., Li, P., & Bai, H. (2013). Tri-band microstrip-fed monopole antenna with dual-polarisation characteristics for WLAN and WiMAX applications. *Electronics Letters, 49*(25), 1597-1598.

[11] Sharma, A., & Gangwar, R. K. (2016). Compact triband cylindrical dielectric resonator antenna with circular slots for wireless application. *Journal of Electromagnetic Waves and Applications, 30*(3), 331-340.

[12] Yang, X., Ge, L., Ji, Y., Zeng, X., Li, Y., Ding, C., ... & Luk, K. M. (2020). An integrated tri-band antenna system with large frequency ratio for WLAN and WiGig applications. *IEEE Transactions on Industrial Electronics, 68*(5), 4529-4540.

[13] Sami, G., Mohanna, M., & Rabeh, M. L. (2013). Tri-band microstrip antenna design for wireless communication applications. *NRIAG Journal of Astronomy and Geophysics, 2*(1), 39-44.

[14] Rajeshkumar, V., & Raghavan, S. (2015). A compact metamaterial inspired triple band antenna for reconfigurable WLAN/WiMAX applications. *AEU-International Journal of Electronics and Communications, 69*(1), 274-280.

[15] Sun, J. S., Fang, H. S., Lin, P. Y., & Chuang, C. S. (2015). Triple-band MIMO antenna for mobile wireless applications. *IEEE Antennas and Wireless propagation letters, 15*, 500-503.

[16] Wu, C. M., Chiu, C. N., & Hsu, C. K. (2006). A new nonuniform meandered and fork-type grounded antenna for triple-band WLAN applications. *IEEE Antennas and Wireless Propagation Letters, 5*, 346-348.

[17] Refaat, S. M., Abdalaziz, A., & Hamad, E. K. (2021). Tri-Band Slot-Loaded Microstrip Antenna for Internet of Things Applications. *Advanced Electromagnetics, 10*(1), 21-28.

[18] Kwak, W. I., Park, S. O., & Kim, J. S. (2006). A folded planar inverted-F antenna for GSM/DCS/Bluetooth triple-band application. *IEEE Antennas and wireless propagation letters, 5*, 18-21.

[19] Liu, W. C., Wu, C. M., & Dai, Y. (2011). Design of triple-frequency microstrip-fed monopole antenna using defected ground structure. *IEEE transactions on antennas and propagation, 59*(7), 2457-2463.

[20] Cui, Y., Luo, P., Gong, Q., & Li, R. (2019). A compact tri-band horizontally polarized omnidirectional antenna for UAV applications. *IEEE Antennas and Wireless Propagation Letters, 18*(4), 601-605.

[21] Koubeissi, M., Mouhamadou, M., Decroze, C., Carsenat, D., & Monédière, T. (2009). Triband compact antenna for multistandard terminals and user's hand effect. *International Journal of Antennas and Propagation, 2009*.

[22] Su, S. W., Lee, C. T., & Chen, S. C. (2018). Compact, printed, tri-band loop antenna with capacitively-driven feed and

end-loaded inductor for notebook computer applications. *IEEE Access, 6*, 6692-6699.

[23] Ding, Y. R., & Cheng, Y. J. (2019). A tri-band shared-aperture antenna for (2.4, 5.2) GHz Wi-Fi application with MIMO function and 60 GHz Wi-Gig application with beam-scanning function. *IEEE Transactions on Antennas and Propagation, 68*(3), 1973-1981.

[24] Zhu, C., Li, T., Li, K., Su, Z. J., Wang, X., Zhai, H. Q., ... & Liang, C. H. (2015). Electrically small metamaterial-inspired tri-band antenna with meta-mode. *IEEE Antennas and Wireless Propagation Letters, 14*, 1738-1741.

[25] Desai, A., Upadhyaya, T., & Palandoken, M. (2018). Dual band slotted transparent resonator for wireless local area network applications. *Microwave and Optical Technology Letters, 60*(12), 3034-3039.

[26] Yazdani, R., Yousefi, M., Aliakbarian, H., Oraizi, H., & Vandenbosch, G. A. (2019). Miniaturized triple-band highly transparent antenna. *IEEE Transactions on Antennas and Propagation, 68*(2), 712-718.

[27] Saeidi, T., Mahmood, S. N., Alani, S., Ali, S. M., Ismail, I., & Alhawari, A. R. (2020, May). Triple-Band Transparent Flexible Antenna for ISM Band and 5G Applications. *In 2020 IEEE International Black Sea Conference on Communications and Networking (BlackSeaCom) (pp. 1-6)*. IEEE.

About Authors

Pankti SHAH received her B. Tech. degree in Electronics and Communication Engineering from Charotar University of Science and Technology, Gujarat, India in May 2021. She has two years of research internship experience in the field of Computer Vision, Antenna and Machine Learning. Currently, she is a graduate student at University of Ottawa in M. Eng. Electrical and Computer Engineering with specialization in Applied Artificial Intelligence. Her current research interest includes AI enabled wireless networks, Chip designing and deep learning, AI supporting electronics designing, Applied machine learning and Computer vision. She is an active member in Google Developer club and Computer Science society.

Yesha PATEL received her B. Tech. degree in Electronics and Communication Engineering from Charotar University of Science and Technology, Gujarat, India in May 2021. Currently, she is working as a Programmer Analyst at Meditab Softwares (I) Pvt. Ltd., Ahmedabad, Gujarat, India. Her current research interests include Transparent antennas, Internet of Things applications. She has published 2 research articles in international conferences based on latest IoT trends. She has remained an active member in IEEE Student Branch, and has served student chair.

Arpan DESAI received his B.E. degree in Electronics and Communication Engineering from Sardar Patel University, Gujarat, India, in 2006; M.Sc. Degree in Wireless Communication Systems from Brunel University, London, United Kingdom in 2008; and a Ph.D. degree from Charotar University of Science and Technology, Gujarat, India in the field of Transparent Antennas in January 2020. Currently, he is working as an Assistant Professor in the Electronics and Communication Engineering Department, Charotar University of Science and Technology, Gujarat, India. His current research interests include transparent antennas, MIMO antennas, energy harvesting devices, transparent DRAs, and flexible wearable antennas. He is serving as a Technical Activity Chair for IEEE Signal Processing Society, Gujarat Section, India and has published more than 45 research articles, mostly in SCI/ Scopus journals, international conferences and book chapters.

Trushit UPADHYAYA received the B.E. degree from Gujarat University, in 2004, the M.E. degree from the Institute of Telecommunication Research, University of South Australia, Adelaide, in 2007, and the Ph.D. degree in satellite antennas from the Charotar University of Science and Technology (CHARUSAT),

Changa, in 2014. He was a Visiting Scientist with the Physical Research Laboratory (PRL), Ahmedabad. He is currently working as a Professor and the Head of Department with the Department of Electronics and Communication Engineering, Faculty of Technology and Engineering, CHARUSAT. His research interests include antenna system design and applied electromagnetics. He has carried out research and consultancy projects for Australian defense agencies, Indian Space Research Organization (ISRO), Gujarat Council on Science and Technology (GUJCOST), and private organizations. He has published and presented several research articles in his area of research in India and abroad and he has delivered invited talk at various organizations across Gujarat.

Merih PALANDOKEN received the M.S. degree study in Microelectronics and Microsystems Engineering from the Technical University of Hamburg, Hamburg, Germany, in 2005 under DAAD scholarship and Ph.D. degree in Theoretical Electrical Engineering from Technical University of Berlin, Germany in 2012. He is currently working in the department of Electrical and Electronics Engineering at Izmir Katip Celebi University as vice head of department. His research interests are analytical/numerical design and modeling of active/passive wireless components in the micro/millimeter wave frequencies especially in the field of RF energy harvesting systems, compact microwave absorbers, machine learning based smart RF component and IoT compatible sensor design, microwave probe design, electrically small bio implantable antennas and RFID systems. He is working as the vice heads of Artificial Intelligence and Data Science Research and Application Center and Smart Factory Systems Research and Application Center at Izmir Katip Celebi University.